Thermodynamic Basis for the Stabilities of Three CutA1s from *Pyrococcus horikoshii, Thermus thermophilus*, and *Oryza sativa*, with Unusually High Denaturation Temperatures†

Masahide Sawano,‡ Hitoshi Yamamoto,‡ Kyoko Ogasahara,§ Shun-ichi Kidokoro,|| Shizue Katoh,⊥ Takayuki Ohnuma,⊥ Etsuko Katoh,⊥ Shigeyuki Yokoyama,‡,#,▽ and Katsuhide Yutani*,‡

RIKEN SPring-8 Center, Harima Institute, 1-1-1 Kouto, Sayo, Hyogo 679-5148, Japan, Institute for Protein Research, Osaka University, 3-2 Yamada-oka, Suita, Osaka, 565-0871, Japan, National Institute of Agrobiological Sciences, 2-1-2 Kannondai, Tsukuba, Ibaraki 305-0856, Japan, Department of Bioengineering, Nagaoka University of Technology, 1603-1 Kamitomioka-cho, Nagaoka, Niigata 940-2188, Japan, RIKEN Genomic Sciences Center, 1-7-22 Suehiro, Tsurumi, Yokohama 230-0045, Japan, and Graduate School of Science, the University of Tokyo, 7-3-1 Hongo, Bunkyo-ku, Tokyo, 113-0033, Japan

Received August 29, 2007; Revised Manuscript Received November 14, 2007

ABSTRACT: In order to elucidate the stabilization mechanism of CutA1 from *Pyrococcus horikoshii* (*Ph*CutA1) with a denaturation temperature of nearly 150 °C, GuHCl denaturation and heat denaturation were examined at neutral and acidic pHs. As a comparison, CutA1 proteins from *Thermus thermophilus* (*Tt*CutA1) and *Oryza sativa* (*Os*CutA1) were also examined, which have lower optimum growth temperatures of 75 and 28 °C, respectively, than that (98 °C) of *P. horikoshii*. GuHCl-induced unfolding and refolding curves of the three proteins showed hysteresis effects due to an unusually slow unfolding rate. The midpoints of refolding for *Ph*CutA1, *Tt*CutA1 and *Os*CutA1 were 5.7 M, 3.3 M, and 2.3 M GuHCl, respectively, at pH 8.0 and 37 °C. DSC experiments with *Tt*CutA1 and *Os*CutA1 showed that the denaturation temperatures were remarkably high, 112.8 and 97.3 °C, respectively, at pH 7.0 and that the good heat reversibility was amenable to thermodynamic analyses. At acidic pH, *Tt*CutA1 showed higher stability to both heat and denaturant than *Ph*CutA1. Combined with the data for DSC and denaturant denaturation, the unfolding Gibbs energy of *Ph*CutA1 could be depicted as a function of temperature. It was experimentally revealed that (1) the unusually high stability of *Ph*CutA1 basically originates from a common trimer structure of the three proteins, (2) the stability of *Ph*CutA1 is superior to those of the other two CutA1s over all temperatures above 0 °C at neutral pH, due to the decrease in both enthalpy and entropy, and (3) ion pairs of *Ph*CutA1 contribute to the unusually high stability at neutral pH.

Recently, we have found that the CutA1 from *Pyrococcus horikoshii* (*Ph*CutA1[1]), a hyperthermophile, has a denaturation temperature (T_d) of nearly 150 °C at pH 7.0, as determined using a differential scanning calorimeter (DSC) (*1*). This T_d has exceeded the highest record determined by DSC by about 30 °C. From the structural analyses of CutA1 proteins from three different sources with different growth temperatures (98, 75, and 37 °C), from *Ph*CutA1, *Thermus thermophilus* (*Tt*CutA1), and *Escherichia coli* (*Ec*CutA1), respectively, the stabilization mechanisms have been proposed as follows. The trimer structures (Mw of a monomer: about 12k) of the three proteins are quite similar. The monomeric structure of *Ph*CutA1 seems to be more stabilized by hydrogen bonds, ion pairs, and hydrophobic interactions than the two others. The number of ion pairs in the monomer *Ph*CutA1 is remarkably greater than that of the others (30, 12, and 1 for *Ph*CutA1, *Tt*CutA1, and *Ec*CutA1, respectively). Several ion pairs of *Ph*CutA1 also function at the subunit interface and form ion pair networks in the trimeric structure.

In general, the origin of high stability does not come from a single mechanism but rather results from the combination of several factors such as increases in ion pairs and hydrogen bonds, core hydrophobicity, packing density, the oligomerization of several subunits, and entropic effect (*2*). On the other hand, it has been reported that the ratio of charged residues is much higher in proteins from hyperthermophiles than in those from other sources with lower growth temperatures (*3*), although ion pairs have been known to have negative (*4*, *5*) as well as positive (*6*−*14*) contributions to the conformational stability of proteins. A considerable

† This work was supported in part by Grants-in-Aid No. 17570102 and No. 18031043, and the "National Project for Protein Structural and Functional Analysis" funded by the Ministry of Education, Culture, Sports, Science and Technology of Japan.

* Corresponding author. RIKEN SPring-8 Center, Harima Institute, 1-1-1 Kouto, Sayo, Hyogo 679-5148, Japan. Tel: 81-791-58-2937. Fax: 81-791-58-2917. E-mail: yutani@spring8.or.jp.

‡ RIKEN SPring-8 Center.

§ Osaka University.

|| Nagaoka University of Technology.

⊥ National Institute of Agrobiological Sciences.

RIKEN Genomic Sciences Center.

▽ University of Tokyo.

[1] Abbreviations: *Ph*CutA1, CutA1 from *Pyrococcus horikoshii*; *Tt*CutA1, CutA1 from *Thermus thermophilus*; *Os*CutA1, CutA1 from *Oryza sativa*; GuHCl, guanidine hydrochloride; DSC, differential scanning calorimetry.

10.1021/bi701761m CCC: $40.75
Published on Web 12/22/2007

amount of data is now available on the denaturation experiments with hyperthermophilic proteins (*15*, *16*) and indicates the propensity of the proteins to denature with a very slow rate constant limited by the high kinetic barrier (*17*−*19*). However, the intrinsic character of the extraordinary thermal stability of proteins from hyperthermophiles remains to be elucidated, because thermodynamic analyses of denaturation for hyperthermophile proteins are limited to a few examples (*18*, *20*−*22*). In the case of *Ph*CutA1, the increased number of ion pairs has been suggested by structural analyses to contribute to the stabilization of the trimeric structure and to play an important role in enhancing the T_d, up to 150 °C. Therefore, *Ph*CutA1 is a good sample for physicochemically examining the role of ion bonds in the extremely high stability of a protein from a hyperthermophile.

In this study, in order to elucidate the stabilization mechanism of *Ph*CutA1 with unusually high stability from a thermodynamic viewpoint, we examined the unfolding and refolding of *Ph*CutA1 by a denaturant and heat, which were compared with those of CutA1 proteins from different sources which are *T. thermophilus* and *Oryza sativa* at growth temperatures of 75 and 28 °C, respectively. The stabilization mechanism of *Ph*CutA1 will be discussed from a thermodynamic viewpoint, based on the relationship between the crystal structures of the three proteins and their denaturation experiments.

EXPERIMENTAL PROCEDURES

*Purification of CutA1s from P. horikoshii and T. thermophilus. Ph*CutA1 and *Tt*CutA1 were purified as described previously (*1*). The purified proteins exhibited a single band on SDS−PAGE. The concentration of the proteins was estimated from the absorbance at 280 nm, assuming $E^{1cm}{}_{1\%} = 27.1$ and 13.3, for *Ph*CutA1 and *Tt*CutA1, respectively, which are based on the numbers of aromatic amino acid contents (*23*).

Plasmid Constructs, Expression and Purification of CutA1 from Oryza sativa. The full-length DNA fragments encoding *Os*CutA1, which were fused to an upstream decahistidine (His10) sequence, were cloned using the Gateway system (Invitrogen). The DNA fragments of *Os*CutA1 were prepared by PCR using native *Pfu* DNA polymerase (Stratagene) from rice cDNA (rice full-length cDNA database accession number AK059907). Primers used for *Os*CutA1 amplification were

5′-CACCATCGAAGGTCGTATGGAGTCTACTTCC-3′ and 5′-TTAGCTTTCCCTAGTGCTGTTCTTTAGCC-3′ (the underlined nucleotide sequence corresponds to the factor Xa cleavage site). The full-length PCR products were purified by electrophoresis in a 2% agarose gel using a QIAquick Gel Extraction Kit (Qiagen) and were inserted into a pENTR/SD/D-TOPO vector using a pENTR/SD/D-TOPO Cloning Kit (Invitrogen). The sequence fidelity was confirmed by DNA sequencing. Starting with this entry clone, an expression vector was generated by an LR Reaction Kit (Invitrogen). The *Os*CutA1 was cloned into the pDEST-his vector for expression of the N-terminus His10 fusion proteins (*24*).

For protein production, *Escherichia coli* BL21 (DE3) competent cells (Novagen) were transformed with the expression vector and selected with 50 μg/mL ampicillin. *E. coli* cultures were grown at 37 °C in 500 mL of 2× yeast-tryptone (YT) medium supplemented with 50 μg/mL ampicillin at an absorbance of approximately 0.7 at 600 nm and induced with a final 1 mM isopropyl-1-thio-β-galactopyranoside (IPTG). After 3 h, cells were harvested by centrifugation at 10000*g* for 5 min and the pellets were frozen. The cell pellets were thawed on ice and resuspended in 100 mL of column buffer (50 mM Tris-HCl pH 8.0, 100 mM NaCl) and disrupted by sonication. Lysed cell suspensions were centrifuged at 27000*g* for 30 min at 4 °C.

Soluble His10/*Os*CutA1 protein was loaded directly onto a Ni-bound 5 mL HiTrap Chelating HP column (GE Healthcare Bio-Sciences) equilibrated with column buffer at a flow rate of 5 mL per minute. After washing the column with wash buffer (50 mM Tris-HCl (pH 8.0), 100 mM NaCl, 15 mM imidazole (pH 8.0)), recombinant protein was eluted by increasing the imidazole concentration to 0.4 M. Protein eluted in the presence of 0.4 M imidazole was chromatographed over a HiLoad 26/60 Superdex 75 pg (GE Healthcare Bio-Sciences) that had been equilibrated with column buffer. The purified His10/*Os*CutA1 fusion protein was collected and concentrated to 10 mL using Centriplus YM-10 (Millipore). To remove the region upstream of *Os*CutA1, 8.3 mg of the His10/*Os*CutA1 fusion protein was digested with 6 U of Factor Xa (Novagen) at 37 °C for 16 h. The digestion mixture was eluted over HiLoad 26/60 Superdex 75 pg. The purified proteins exhibited a single band on SDS−PAGE. The concentration of the proteins was estimated from the absorbance at 280 nm, assuming $E^{1cm}{}_{1\%} = 17.9$ for *Os*CutA1, based on the numbers of aromatic amino acid contents (*23*).

DSC Experiments. DSC (differential scanning calorimetry) was carried out using a VP-capillary DSC platform (MicroCal, USA). For the measurements, the protein concentrations were 0.4 to 1.5 mg/mL in 50 mM potassium phosphate, pH 7.0, 50 mM Gly-HCl in the acidic region, or 50 mM Gly-KOH, pH 9.0. All of the samples were filtered through a 0.22-μm pore size membrane after dialysis against the buffers overnight at 4 °C. Analysis of the DSC curves was done using the single two-state transition with a subunit dissociation model (*24*). The denaturation temperature (T_d) means the temperature where the unfolding fraction is 0.5. In eq 7, the T_d was assumed to be close to that at $\Delta G = 0$.

CD Spectra. Circular dichroism (CD) spectra of the three proteins were recorded on a Jasco J-725 spectropolarimeter (Jasco Co., Japan). Far-UV and near-UV CD spectra were scanned 16 times at a scan rate of 20 nm/min, using a time constant of 0.25 s. The light path length of the cell used was 1 or 10 mm in the far-UV region and 10 mm in the near-UV region. For calculation of the mean residue ellipticity, [θ], the mean residue weights of *Ph*CutA1, *Tt*CutA1, and *Os*CutA1 were assumed to be 121.1, 112.8, and 110.8, respectively.

Guanidine Hydrochloride-Induced Unfolding and Refolding. For unfolding, *Ph*CutA1, *Tt*CutA1, and *Os*CutA1 were incubated in GuHCl under various conditions and at different temperatures for various times, except for *Ph*CutA1 at pH 8.0 because it was not denatured even after incubation of 30 min at 120 °C. For refolding, the completely unfolded proteins in the presence of 7 M GuHCl under the following conditions were diluted with 20 mM buffer with 0.1 mM EDTA containing various concentrations of GuHCl. *Ph-*

CutA1 below pH 3.0 was completely unfolded after 1 h incubation at 80 °C in 7 M GuHCl. Therefore, the unfolded protein solution of *Ph*CutA1 at pH 8.0 was prepared by overnight dialysis in the buffer of pH 8.0 in 7 M GuHCl at 4 °C or by jumping to pH 8.0 using concentrated alkaline solution, after 1-h incubation at 80 °C in 7 M GuHCl at pH 2.5. *Tt*CutA1 was completely denatured after 1-h incubation at 80 °C in 7 M GuHCl at a given pH. *Os*CutA1 was completely denatured after 10-min incubation at 80 °C in 7 M GuHCl at pH 8.0.

The unfolding and refolding were monitored by measuring the CD values at 220 nm and at the incubation temperatures of the reactions. CD measurements were carried out with a Jasco J-725 spectropolarimeter. The fraction of unfolding was calculated using eq 1,

$$f_u = (b_n^0 + a_n x - y)/(b_n^0 + a_n x - b_u^0 - a_u x) \quad (1)$$

where f_u is the fraction of the unfolded state, y the CD value at a given concentration of GuHCl, and x the concentration of GuHCl. b_n^0 and b_u^0 are the CD values for the native and the unfolded state at 0 M GuHCl (*17*). Unfolding (refolding) curves were analyzed by the linear extrapolation model assuming a two-state transition for unfolding of a trimer protein, according to eqs 2−6 (see the appendix of Backman et al. (*26*)), in which K, C_t, and $\Delta G°$ are the equilibrium

$$N_3 \leftrightarrow 3U \quad (2)$$

$$K = 27C_t^2 f_u^3/(1 - f_u) \quad (3)$$

$$\Delta G° = -RT \ln K \quad (4)$$

$$\Delta G° = \Delta G°_{H2O} + mx \quad (5)$$

$$f_u = (((1/2)((\exp(-(\Delta G°_{H2O} + mx)/(RT)))/(27C_t^2)) + (1/18)((\exp(-(\Delta G°_{H2O} + mx)/(RT)))/(27C_t^2))(4((\exp(-(\Delta G°_{H2O} + mx)/(RT)))/(27C_t^2)) + 27)^{1/2}3^{1/2})^{1/3} - (1/3)((\exp(-(\Delta G°_{H2O} + mx)/(RT)))/(27C_t^2))/((1/2)((\exp(-(\Delta G°_{H2O} + mx)/(RT)))/(27C_t^2)) + (1/18)((\exp(-(\Delta G°_{H2O} + mx)/(RT)))/(27C_t^2))(4((\exp(-(\Delta G°_{H2O} + mx)/(RT)))/(27C_t^2)) + 27)^{1/2}3^{1/2})^{1/3}) \quad (6)$$

constant of the unfolding reaction, the molar concentration of the protein expressed in trimer equivalents, and the Gibbs energy change upon unfolding (standard value), respectively. Factor m is the slope of the linear correlation between $\Delta G°$ and the GuHCl concentration (x). $\Delta G°_{H2O}$ is the standard value in the absence of GuHCl (in water) which is independent of the examined protein concentration. Factor f_u in eq 6 is represented as a function of the concentration of GuHCl. We used data analysis software from OriginLab (Northampton, MA) to produce a least-squares fit of the experimental data in the GuHCl unfolding curves to eq 6 to obtain $\Delta G°_{H2O}$.

Analytical Ultracentrifugation. Equilibrium sedimentation experiments were performed on a Beckmann Coulter XL-A (Fullerton, CA). All experiments were run at 20 °C using an An-60 Ti rotor at a speed of 20,000 rpm. Before measurements were taken, the protein solutions were dialyzed overnight against each buffer at 4 °C. The experiments at three different protein concentrations between 0.4 and 0.1 mg·mL^{-1} were run in Beckman 4-sector cells. The partial specific volumes of 0.748, 0.757, and 0.748 cm^3·g^{-1} for *Ph*CutA1, *Tt*CutA1, and *Os*CutA1, respectively, were calculated from the amino acid compositions (*27*). Analysis of the sedimentation equilibrium was performed using the program Beckman XL-A/XL-I Data analysis software ver4.

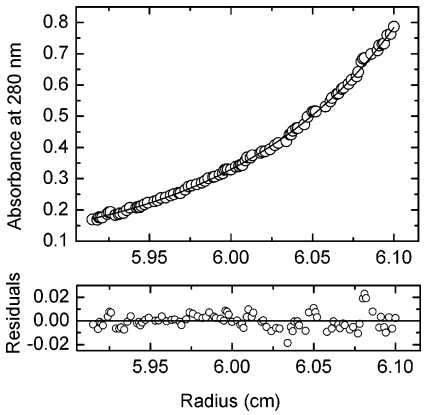

FIGURE 1: Sedimentation equilibrium analysis of *Ph*CutA1 at pH 7.0 and 20 °C. The sedimentation equilibrium experiment was performed at the protein concentration of 0.15 mg·mL^{-1} in 50 mM potassium phosphate buffer pH 7.0 containing 10 mM EDTA and 100 mM NaCl at 20 °C. The solid line drawn through the data was obtained by fitting for a single ideal species. The residuals (difference between the experimental data and the fitted data for each point) are shown in the bottom panel. The apparent molecular weight was 35,300.

Table 1: Apparent Molecular Weights of *Ph*CutA1, *Tt*CutA1, and *Os*CutA1 at Various pHs and 20 °C

		MW[a] × 10^{-3}			
proteins	additive	pH 2.5	pH 7.0	pH 9.0	MW of a trimer[b]
*Ph*CutA1	10 mM EDTA[c]	37.0	35.8	35.4	37.044
	1.0 M GuHCl		36.2	35.8	
*Tt*CutA1	10 mM EDTA[c]	34.8	47.5	32.6	34.866
*Os*CutA1	10 mM EDTA		37.4		37.572

[a] Molecular weights represent average values at three different concentrations of proteins. [b] This means MW calculated from amino acid compositions. [c] Protein solution at pH 2.5 does not contain 10 mM EDTA.

RESULTS

Molecular Assembly Forms of the Three CutA1s at Different pHs. The assembly forms of *Ph*CutA1, *Tt*CutA1, and *Os*CutA1 were examined by sedimentation equilibrium experiments at 20 °C, because the X-ray analysis of *Ph*CutA1 suggests heavy metal-induced multimerization of a protein (*28*). The sedimentation patterns of *Ph*CutA1 at pH 7.0 were fitted to an analysis of a single species with a molecular weight of 35.3 k as shown in Figure 1, suggesting a homogeneous molecular mass distribution in the solution. Similar results were observed for the three proteins at various pHs. The apparent molecular weights of the three proteins at various pHs are presented in Table 1. These values correspond to three times a monomer calculated from the amino acid sequences; 37,044 for *Ph*CutA1, 34,866 for *Tt*CutA1 and 37,572 for *Os*CutA1, indicating that all of the CutA1s have a trimeric form composed of identical subunits in the pH region between 2.5 and 9.0. Although the apparent molecular weights of *Tt*CutA1 at 7.0 were slightly higher

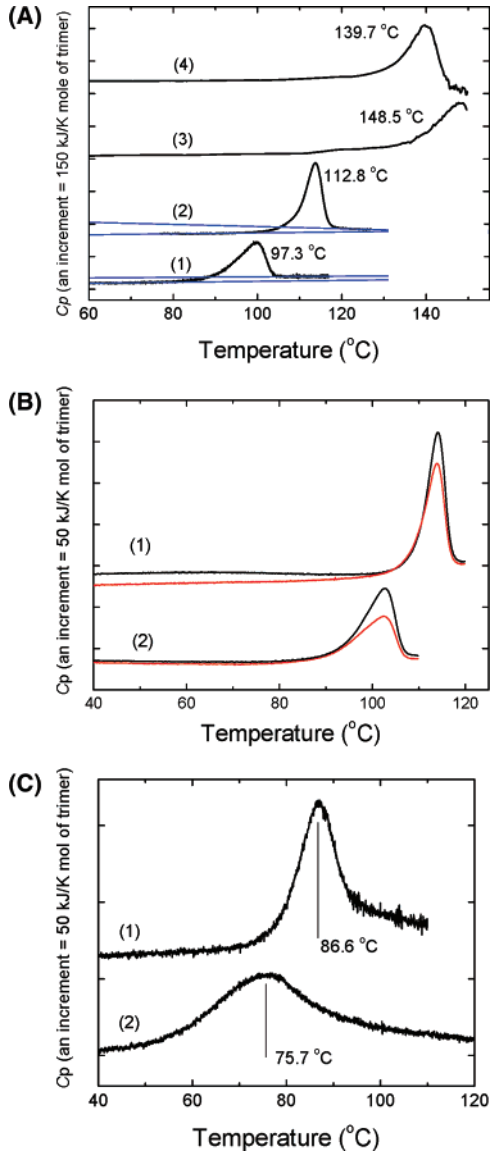

FIGURE 2: Typical excess heat capacity curves of three CutA1 proteins. (A) Curves (1), (2), (3), and (4) represent DSC curves at a scan rate of 60 °C/h of *Os*CutA1 at pH 7.0, *Tt*CutA1 at pH 7.0, *Ph*CutA1 at pH 7.0, and *Ph*CutA1 at pH 9.0, respectively. Curves (3) and (4) are cited from Tanaka et al. (*1*). The blue lines of curves (1) and (2) denote the baseline used for the ΔH calculation. (B) Reversibilities of heat denaturation for *Tt*CutA1 (1) and *Os*CutA1 (2) at pH 7.0. DSC curves were obtained at scan rates of 200 °C/h. Red curves in curves (1) and (2) are the second runs of DSC just after cooling of the first run (black curves), in which the recovery area of excess heat capacity was 90 and 81%, respectively. (C) Comparison of heat stability for *Tt*CutA1 (1) and *Ph*CutA1 (2) at pH 2.5. The scan rates of both DSC curves were 60 °C/h. The peak temperatures of *Tt*CutA1 and *Ph*CutA1 were 86.6 and 75.5 °C, respectively.

than that of the trimer, the molecular weight extrapolated to zero concentration was $(33.4 \pm 0.3) \times 10^3$, using the software (utility mw vs concentration) supplied by the manufacturer. These results indicate that all of *Ph*CutA1, *Tt*CutA1 and *Os*CutA1 might exist predominantly in a trimeric form. Therefore, we assumed the equilibrium ($N_3 \leftrightarrow 3U$) between a trimer in the native state (N_3) and a monomer in the denatured state (3U) for analyzing the following DSC curves, and unfolding and refolding reactions due to denaturant denaturation.

DSC Experiments of Three CutA1 Proteins. Figure 2A shows the DSC curve of *Os*CutA1 at pH 7.0, with DSC curves of the other two proteins already reported (*1*). The denaturation temperature (T_d) of *Os*CutA1 was considerably high, 97.3 °C, compared with the optimum growth temperature (28 °C) of the plant. This large difference between T_d and the optimum growth temperature is coincident with the cases of *Ph*CutA1 and *Tt*CutA1, suggesting that these unusual stabilities are a common characteristic of CutA1, the function of which remains to be elucidated. At pH 9.0 the T_d values for *Tt*CutA1 and *Os*CutA1 were similar to the results at pH 7.0, but that for *Ph*CutA1 was lower (Figure 2A).

To examine the reversibility of heat denaturation, the second runs of DSC were performed just after cooling of the first run, and the recovery area of excess heat capacity due to heat denaturation was measured. The heat reversibility of *Tt*CutA1 was considerably good even though the T_d was over 110 °C around neutral pH: the recovery rates were 57 and 90% at scan rates of 60 and 200 °C/h, respectively (curve (1) of Figure 2B), although the heat denaturation of *Ph*CutA1 with a denaturation temperature of nearly 150 °C is completely irreversible at neutral pH as shown in our previous paper (*1*). The scan rate dependence of the T_d for *Tt*CutA1 was hardly detected at 60 and 45 °C/h around neutral pH, although it was slightly detected at 60 and 200 °C/h. Therefore, we used the scan rate of 60 °C/h for the calculation of unfolding enthalpies (ΔH_d). The ΔH_d of *Tt*CutA1 was 1777 kJ/mol of a trimer at 112.8 °C at pH 7.0. In the case of *Os*CutA1 (Figure 2B), the recovery of the area of excess heat capacity due to heat denaturation was 44 and 81% at scan rates of 60 and 200 °C/h, respectively, at pH 7.0. The ΔH_d of *Os*CutA1 was 1453 kJ/mol of a trimer at 97.3 °C at pH 7.0 (scan rate of 60 °C/h). The difference in the apparent recovery of the DSC curves depending on the scan rate might be caused by that the unfolded proteins after heat denaturation irreversibly associate depending on the incubation time at the high temperatures.

DSC experiments could not be done near the isoionic point of these proteins (around pH 5) due to aggregation after heat denaturation. However, in the more acidic region, the DSC curves of both *Ph*CutA1 and *Tt*CutA1 could be observed, but that of *Os*CutA1 was not seen, suggesting acidic denaturation. In the acidic region, where ion pairs have completely disappeared due to protonation, it is important to examine the stability of *Ph*CutA1, speculated to be stabilized by ion pairs. As expected, the peak temperature of *Ph*CutA1 was lower than that of *Tt*CutA1; for example, 75.7 and 86.6 °C at pH 2.5, respectively (Figure 2C). This indicates that the stability of *Tt*CutA1 is superior in the acidic region, the T_d of which was over 35 °C less than that of *Ph*CutA1 at pH 7.0. This means that the protein from an extreme thermophile is more stable than that from a hyperthermophile at acidic pH.

CD Spectra of the Three Proteins. The near-UV CD spectrum of *Ph*CutA1 shows a bigger positive peak around 280 nm than those of the other two proteins (Figure 3A), which is caused by a bigger amount of Trp and Tyr residues (5 + 4, 2 + 3, and 3 + 4 for Trp + Tyr of *Ph*CutA1, *Tt*CutA1, and *Os*CutA1, respectively). A peak around 245 nm was observed for *Ph*CutA1, which could not be assigned. There is one Cys each and no disulfide bond in the three

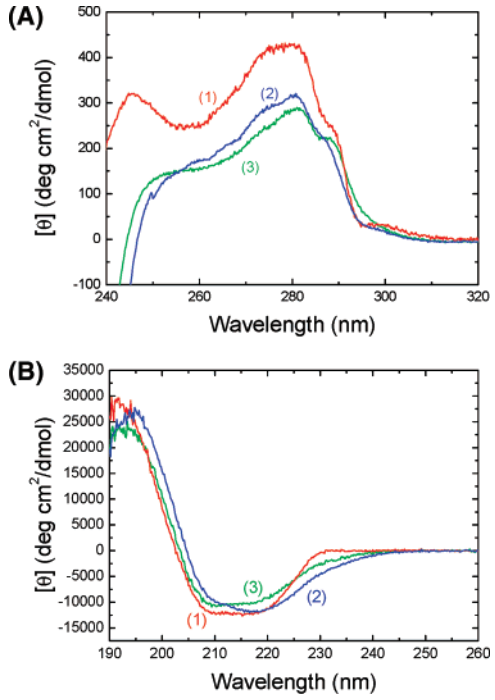

FIGURE 3: Near- (A) and far-UV (B) CD spectra of *Ph*CutA1, *Tt*CutA1, and *Os*CutA1at pH 7.0 and 25 °C. Spectra (1), (2), and (3) represent the CD spectra of *Ph*CutA1, *Tt*CutA1, and *Os*CutA1, respectively.

proteins, although the Cys residue of *Ph*CutA1 is transformed into cystein-s-dioxide in the crystal structure (PDB ID; 1V99).

The far-UV CD spectra of the three proteins were nearly similar as shown in Figure 3B, corresponding to the similar backbone structures shown by X-ray analyses. The structure of *Os*CutA1 has also been determined to be similar to that of the other two proteins as reported elsewhere (private communication). Because far-UV CD spectra of a protein have been affected due to the aromatic residues (*29*), the differences in far-UV CD spectra of the three proteins might be caused mainly by differences in the content of aromatic residues.

GuHCl-Induced Unfolding and Refolding at pH 8.0 and 37 °C. At neutral pH, the CD spectrum in the far-UV region of *Ph*CutA1 was not affected even after 30-min incubation at 120 °C in 7 M GuHCl, indicating that the protein still retains the native conformation. However, after denaturation treatment in the acidic region as described in Experimental Procedures, the refolding curves as a function of GuHCl concentration were detected at pH 8.0 and 37 °C as shown in Figure 4A. The midpoints of refolding moved slightly to higher concentrations of GuHCl depending on the incubation days and attained constant values after 28 days at 37 °C, which was in 5.7 M GuHCl. This slow refolding rate might be correlated with the fact that the unfolding rate of *Ph*CutA1 is too slow for the unfolding to be detected under neutral pHs even in 7 M GuHCl. It has been reported for the protein from *P. furiosus*, a hyperthermophile, that both unfolding and refolding rates are unusually slow (*18*).

In the case of *Tt*CutA1, the unfolding proceeded slowly, especially in the concentrations around transition points (5.5 M GuHCl) as shown in Figure 4B: the midpoints of unfolding were 5.8, 5.5, 5.4, 5.3, and 5.2 M after 1-, 4-, 7-, 14-, and 28-day incubation at pH 8.0 and 37 °C, respectively. The refolding also proceeded slowly, but attained a constant value after 7 days: the midpoints of refolding were 3.3, 3.3, 3.4, and 3.4 M for 1-, 2-, 7-, and 14-day incubation, respectively, after the dilution at pH 8.0 and 37 °C. These results indicate that the unfolding and refolding reaction of *Tt*CutA1 cannot attain the same values in several weeks or that there is hysteresis in both reactions.

The refolding reaction of *Os*CutA1 apparently reached constant values in 1 day at pH 8.0 and 37 °C, although the midpoints of unfolding depended on the incubation days and were 3.8, 3.4, and 3.3 M for 1, 7, and 14 days, respectively. As shown in Figure 4C, the unfolding and refolding curves of *Os*CutA1 were also clearly different. These results indicate that all the CutA1 proteins from different sources show apparently similar behavior in the unfolding and refolding reactions with apparent hysteresis arising from the slow unfolding reaction described below, although the midpoints of refolding for *Os*CutA1, *Tt*CutA1, and *Ph*CutA1were remarkably different, being 2.3 M after 1 day, 3.3 M after 7 days, and 5.7 M after 28 days, respectively, which attained almost constant values (Figure 4D). Figure 4D represents the normalized refolding curves of the three proteins, from which the data were used for the fitting of eq 6. These differences in midpoints of denaturant denaturation among the three proteins correspond to the differences in the denaturation temperatures of heat denaturation.

GuHCl-Induced Unfolding and Refolding in the Acidic Region at 37 °C. In the acidic region, the heat stabilities of *Ph*CutA1 and *Tt*CutA1 remarkably decreased compared with those at neutral pH (Figure 2). *Os*CutA1 was almost completely denatured below pH 2.5. To examine the stabilities by denaturant of *Ph*CutA1 and *Tt*CutA1 in the acid region, the GuHCl unfolding and refolding were examined at pH 2.5 and 37 °C. As shown in Figure 5A the midpoints of the unfolding and refolding curves of *Ph*CutA1 were almost the same (3.7 M GuHCl) after 1 day at 37 °C, meaning that they attained equilibrium. On the other hand, the midpoints of the unfolding and refolding curves of *Tt*CutA1 were slightly different and were 4.1 and 3.8 M after 1 day at 37 °C, respectively (Figure 5B). These results indicate that *Tt*CutA1 is stabler than *Ph*CutA1 at pH 2.5 (Table 3) in agreement with DSC results and that the apparent hysteresis at neutral pH might be caused by the abnormally slow denaturation rate of CutA1s because the apparent hysteresis almost disappears under unstable conditions at pH 2.5 but slightly remains for *Tt*CutA1 which is stabler than *Ph*CutA1.

Confirmation of Recoveries of Proteins Refolded from Denaturant Denaturation. As shown in Figures 4 and 5, the CD values of all three CutA1 proteins refolded from concentrated denaturants were 80−90% of the native ones, indicating that the recoveries were not completed. Therefore, we examined whether intermediates or impurities were included in the refolded proteins. We found by gel-filtration that there were aggregated ones in the refolded proteins of *Ph*CutA1 and *Tt*CutA1. The main peaks of the gel-filtration products were quantitatively examined by CD spectra and DSC experiments, and it was confirmed that the refolded ones of *Ph*CutA1 and *Tt*CutA1 are the same as those of the intact proteins (not shown). As shown in the refolding data of Figures 4A, 4B, and 4C, a continuous decrease in negative CD values was not observed for long days in the refolding

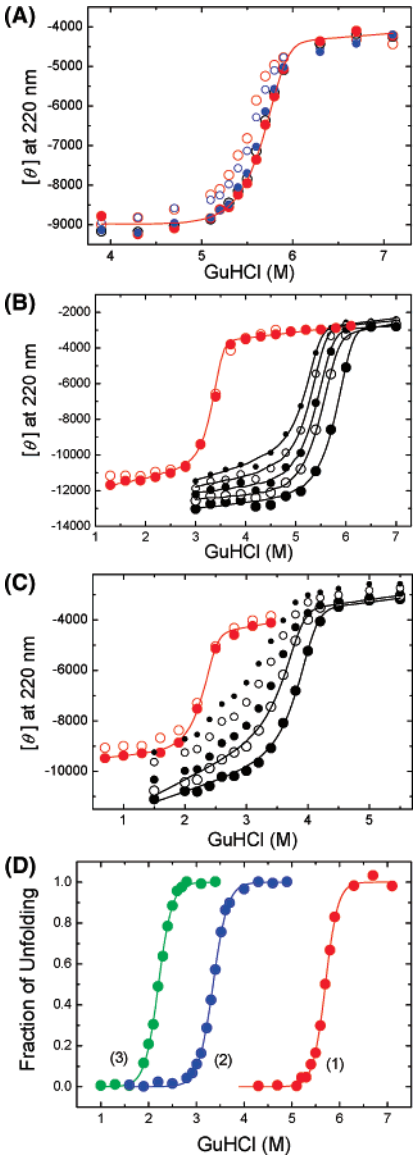

FIGURE 4: GuHCl-induced unfolding and refolding curves of *Ph*CutA1, *Tt*CutA1, and *Os*CutA1 at pH 8.0 and 37 °C. The unfolding and refolding were monitored by the CD values at 220 nm. (A) Refolding points of *Ph*CutA1 as a function of GuHCl concentration after 1-, 2-, 7-, 14-, and 28-day incubation are represented by red open, small blue open, small blue closed, blue open, and red closed circles, respectively. Red fitting line was obtained from 28-day incubation. (B) Unfolding points of *Tt*CutA1 after 1-, 4-, 7-, 14-, and 28-day incubation are shown by black big closed, black big open, black closed, black open, and black small closed circles, respectively. Red open and closed circles represent the refolding plots after 1- and 7-day incubation, respectively. Red fitting line was obtained from 7-day incubation. (C) Unfolding points of *Os*CutA1 after 1-, 4-, 7-, 14-, and 28-day incubation are shown by black big closed, black big open, black closed, black open, and black small closed circles, respectively, and the midpoints of the black fitting line after 1- and 4-day incubation were 3.9 and 3.6, respectively. Red closed and open circles represent the refolding plots after 1- and 2-day incubation, respectively. Red fitting line was obtained from 1-day incubation. (D) Normalized refolding curves of the three proteins as a function of GuHCl concentration calculated according to eq 1. Curves (1), (2), and (3) represent the refolding curves of *Ph*CutA1 after 28-day incubation, *Tt*CutA1 after 7-day incubation, and *Os*CutA1 after 1-day incubation at pH 8.0 and 37 °C, with the midpoints of 5.7, 3.3, and 2.3 M GuHCl, respectively. These normalized values were fitted to eq 6 to obtain the unfolding ΔG°_{H2O} values in Table 3. The obtained parameters were recalculated to produce the lines in Figure 4 (A), (B), and (C) and Figure 5 (A) and (B).

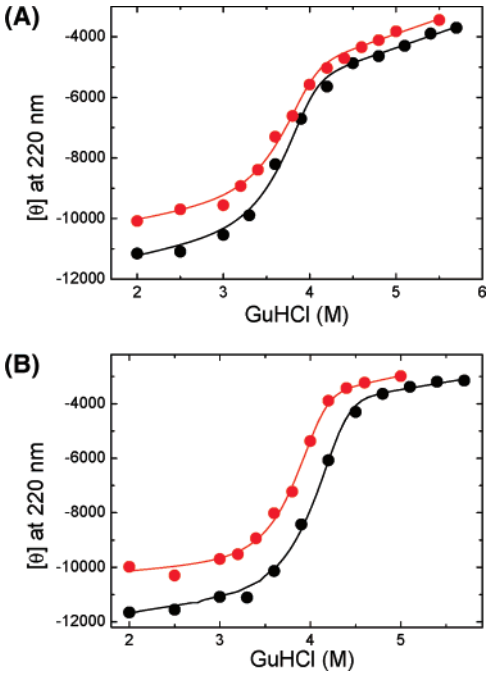

FIGURE 5: GuHCl-induced unfolding and refolding curves of *Ph*CutA1 and *Tt*CutA1 at pH 2.5 and 37 °C. Black and red circles represent unfolding and refolding data, respectively, after 1-day incubation. (A) *Ph*CutA1 monitored at 220 nm. The midpoints of refolding and unfolding of *Ph*CutA1 were nearly the same, 3.8 M GuHCl. (B) *Tt*CutA1 at 220 nm. The midpoints of refolding and unfolding of *Tt*CutA1 were 3.8 and 4.1 M GuHCl, respectively. Other fitting parameters are listed in Table 3.

process at pH 8.0, suggesting that aggregation might occur in the initial step of refolding. As shown in the unfolding data of Figure 4B and 4C, however, negative CD values decreased depending on the incubation days. This suggests that refolding data attaining constant values are amenable to thermodynamic analyses of refolding curves assuming that aggregated proteins can be excluded in the initial step of refolding. However, data for the unfolding curves at pH 8.0 were not amenable to such an analysis because the data did not attain equilibrium.

DISCUSSION

Hysteresis of Unfolding and Refolding Curves. All three CutA1s were confirmed by analytical ultracentrifugation to be trimers in solution in the examined pH region between 2.5 and 9.0. GuHCl-induced unfolding and refolding curves for *Tt*CutA1 and *Os*CutA1 did not coincide at pH 8.0 and 37 °C (Figures 4 B and C). The midpoint of refolding of *Ph*CutA1 was 5.7 M after 28-day incubation at pH 8.0 and 37 °C, although the unfolding curves were not detected. These results indicate that the unfolding and refolding of the three proteins show hysteresis effects. The refolded *Ph*CutA1 and *Tt*CutA1 were verified to be intact from the fact that the refolded proteins showed the same denaturation temperatures and CD spectra as those of the native ones. This means that the hysteresis is not caused by the formation of alternatively folded structures or any intermediates during refolding. Furthermore, at acidic pH 2.5, the midpoints of the unfolding and refolding curves of *Ph*CutA1 were almost the same, although those of *Tt*CutA1 are still slightly different (Table 3). These results suggest that the hysteresis is caused by the unusually slow unfolding rate. Although *Tt*CutA1 and

Table 2: Thermodynamic Parameters at Denaturation Temperature Obtained from DSC Experiments for Three CutA1 Proteins at pH 7.0

		ΔC_p (kJ/mol/K)		ΔH at T_d (kJ/mol)		ΔG at 97.3 °C (kJ/mol)		ΔH at 97.3 °C (kJ/mol)	
proteins	T_d (°C)	A[a]	B[a]	A	B	A	B	A	B
*Ph*CutA1	148.5	18.3	24.0	1959[b]	2310[b]	178.8[b]	202.2[b]	1023[b]	1081[b]
*Tt*CutA1	112.8	17.3	23.6	1777		65.9[b]	64.7[b]	1509[b]	1411[b]
*Os*CutA1	97.3	17.4	22.9	1453		0		1453	

[a] A and B mean ΔC_p values calculated from each crystal structure using parameters of Murphy and Freire (*33*) amd Spolar et al. (*34*), respectively. [b] Estimated values using ΔC_p values of A or B.

Table 3: Thermodynamic Analyses of Conformational Stability from GuHCl Unfolding/Refolding Curves for Three CutA1 Proteins at 37 °C

proteins	conditions	concentration (μM)	$\Delta G°_{H2O}$[a] (kJ/mol)	midpoint (M)	slope (m) (kJ/mol M)	effective ΔG_{H2O}[a] (kJ/mol)
*Ph*CutA1	pH 2.5, ref,[b] 1 day	0.54	153.9 ± 9.3	3.69 ± 0.02	−22.9 ± 2.5	
	pH 2.5, unf,[b] 1 day	0.54	160.6 ± 12.7	3.70 ± 0.03	−24.6 ± 2.6	
	pH 8, ref, 28 days	0.54	271.3 ± 3.3	5.68 ± 0.01	−35.4 ± 1.8	220.4
*Tt*CutA1	pH 2.5, ref,[b] 1 day	0.62	171.9 ± 9.2	3.84 ± 0.01	−26.9 ± 1.8	
	pH 2.5, unf,[b] 1 day	0.62	173.2 ± 9.2	4.06 ± 0.01	−25.5 ± 1.7	
	pH 8, ref,[b] 7 day	0.62	207.7 ± 8.4	3.33 ± 0.01	−41.2 ± 1.8	156.8
*Os*CutA1	pH 8, ref,[b] 1 day	0.44	158.1 ± 2.9	2.30 ± 0.01	−38.1 ± 2.2	107.2

[a] $\Delta G°_{H2O}$ is the standard value obtained using eq 6, which is independent of the examined protein concentration. Effective ΔG_{H2O} means values at protein concentration of 0.02 mM which is close to protein concentration used in DSC experiments. [b] "ref" and "unf" represent the analyses from refolding and unfolding curves, respectively.

*Os*CutA1 did not attain equilibrium due to a very slow unfolding rate at pH 8, the three proteins in the refolding process seemed to attain constant values as shown in Figure 4 (A), (B), and (C). Refolding in heat denaturation by DSC for three proteins was observed from the second run just after the first run of the DSC experiments, suggesting that the refolding rate is not abnormal compared with the fact that pyrrolidone carboxyl peptidase from a hyperthermophile, *Pyrococcus furiosus*, takes about 1 day at 30 °C in the acidic pH for recovery from heat denaturation (*18*). These results suggest that the constant values obtained from refolding experiments are close to equilibrium so that the data can be amenable to thermodynamic analyses.

There are several reports of hysteresis in the dimeric luciferase β-subunit after urea denaturation (*30*), tetrameric transthyretin after GuHCl denaturation (*31*), and dimeric creatine kinase after urea denaturation (*32*). Their causes have not been revealed in detail.

Temperature Dependences of Unfolding Gibbs Energy (Stability Curves) of Three CutA1 Proteins. It is generally difficult to observe the heat reversibility of proteins with high denaturation temperatures around 100 °C at neutral pH due to the formation of aggregation following heat denaturation. The DSC curves of *Tt*CutA1 and *Os*CutA1 showed considerably good reversibility at neutral pH, even though the denaturation temperatures were remarkably high (113 and 97 °C, respectively). These results suggest that the area of excess heat capacities induced by heat denaturation under these conditions shows the real enthalpy change of unfolding (ΔH_d) at the denaturation temperature. However, it was difficult to experimentally obtain heat capacity change (ΔC_p) using ΔH values at different denaturation temperatures measured at different pHs because the DSC experiments could not be done near the isoionic point of these proteins (around pH 5) due to aggregation after heat denaturation. Therefore, the ΔC_p values of *Tt*CutA1 and *Os*CutA1at neutral pH were estimated from the method induced by the burial surface area of amino acid residues from the crystal structure, the parameters of which are given by two groups, Murphy and Freire (*33*) and Spolar et al. (*34*).

If we can obtain thermodynamic parameters such as ΔH_d, T_d, and ΔC_p, the Gibbs energy of unfolding (ΔG) can be expressed as a function of temperature as follows (*35*):

$$\Delta G = \Delta H_d + \Delta C_p(T - T_d) - T(\Delta H_d/T_d + \Delta C_p \ln(T/T_d)) \quad (7)$$

where ΔH_d is the enthalpy at T_d, and ΔC_p is constant in the regarded temperature range. Figure 6 shows the temperature functions of ΔG for *Tt*CutA1 and *Os*CutA1 at pH 7.0. The different parameters of ΔC_p from the above two groups (*33*, *34*) were used.

The three CutA1 proteins were confirmed as to be trimeric proteins in solution (Table 1). The refolding curves of the three proteins at pH 8 seemed to attain constant values, and the unfolding and refolding curves at pH 2.5 nearly coincided in the cases of both *Ph*CutA1 and *Tt*CutA1. Therefore, the GuHCl-induced unfolding and refolding curves were analyzed based on a two-state model for a trimeric protein ($N_3 \leftrightarrow 3U$) using eq 6. By fitting the normalized data such as Figure 4D to eq 6, $\Delta G°_{H2O}$ values were obtained. The calculated thermodynamic parameters are listed in Table 3. The denaturation curves depend on protein concentration, because CutA1 proteins are oligomeric proteins. The ΔG_{H2O} values at a given concentration (C_t) can be expressed as follows when a protein is a trimer (*24*),

$$\Delta G_{H2O} = \Delta G°_{H2O} + RT \ln(C_t^2) \quad (8)$$

where $\Delta G°_{H2O}$ is the standard value. The effective ΔG_{H2O} in Table 3 show values at a protein concentration (0.02 mM for a trimer) close to the protein concentrations used in the DSC experiments. In these fitting calculations, the standard deviations were around 0.5−1% for C_m (midpoint of denaturation) and approximately 5−10% for $\Delta G°_{H2O}$, which are similar to reported values (*26*).

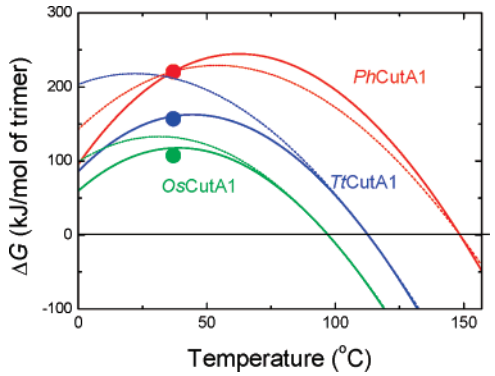

FIGURE 6: Temperature functions of unfolding Gibbs energy for the three CutA1 proteins at neutral pH. The red, blue, and green circles represent the effective ΔG_{H2O} values of *Ph*CutA1, *Tt*CutA1, and *Os*CutA1, respectively, at pH 8.0 and 37 °C, which were obtained from the GuHCl denaturation curves at a protein concentration of 0.02 mM close to the protein concentration in the DSC experiments. The solid blue curve represents the temperature dependence of ΔG of *Th*CutA1 at pH 7.0 using the thermodynamic parameters of ΔH (1777 kJ/mol), ΔC_p (23.6 kJ/mol/K), and T_d (112.8 °C) and the dotted blue curve using the thermodynamic parameters of ΔH (1777 kJ/mol), ΔC_p (17.3 kJ/mol/K), and T_d (112.8 °C). The solid green curve, *Os*CutA1 at pH 7.0 using the thermodynamic parameters of ΔH (1453 kJ/mol), ΔC_p (22.9 kJ/mol/K), and T_d (97.3 °C) and the dotted green curve using the thermodynamic parameters of ΔH (1453 kJ/mol), ΔC_p (17.4 kJ/mol/K), and T_d (97.3 °C). The solid red curve, *Ph*CutA1 at pH 7.0 using the thermodynamic parameters of ΔH (2310 kJ/mol), ΔC_p (24.0 kJ/mol/K), and T_d (148.5 °C) and the dotted red curve, *Ph*CutA1 at pH 7.0 using the thermodynamic parameters of ΔH (1959 kJ/mol), ΔC_p (18.3 kJ/mol/K), and T_d (148.5 °C). The ΔH values used for*Tt*CutA1 and *Os*CutA1 and the T_d values for three proteins were the experimental data, and the other parameters were the derived ones (Table 2 and Table 3).

In the neutral pH region, the effective ΔG_{H2O} values for *Tt*CutA1 and *Os*CutA1 were close to the unfolding ΔG curve versus temperature obtained from the DSC experiments as shown in the solid curves of blue (*Tt*CutA1) and green (*Os*CutA1) in Figure 6 when the parameters of ΔC_p from Spolar et al. (*34*) were used. Although they are slightly different when the other parameters (*33*) were used, these comparisons might be meaningful. The good agreement of the former case should result from the good quality of the DSC data with a high reversibility even around 100 °C. However, *Ph*CutA1 with the denaturation temperature of 148.5 °C did not precisely show the unfolding enthalpy (ΔH_d) for two reasons: (1) the thermal transition was not completed due to the temperature limit (150 °C) of the machine and (2) the protein was partially aggregated by heat denaturation. Thus, we estimated ΔH_d at 148.5 °C using the effective ΔG_{H2O} (220.4 kJ/mol) obtained from the refolding curves at 37 °C (Table 3) to be 1959 or 2310 kJ/mol for the ΔC_p of 18.3 or 24.0 kJ/mol/K, respectively (Table 2), which are estimated from the crystal structure (*33*, *34*). The red solid and dotted curves in Figure 6 were depicted using these thermodynamic parameters of *Ph*CutA1. These results indicate that the unusually high stability of *Ph*CutA1 is practically superior to those of the other two CutA1s in the range of all temperatures over zero °C.

The Mechanism of Stabilization of PhCutA1 with Extremely High Stability. *Ph*CutA1 with a denaturation temperature of nearly 150 °C at pH 7.0 was not denatured even after 30 min incubation in 7 M GuHCl at 120 °C, judging from the CD spectra in the far-UV region. The unfolded *Ph*CutA1 after 1-h incubation at 80 °C in 7 M GuHCl at pH 2.5 was completely refolded at pH 8.0 and 37 °C. The midpoint of the refolding curve was 5.7 M GuHCl. On the other hand, *Tt*CutA1 and *Os*CutA1 in comparison with *Ph*CutA1 also showed high stability to both heat and the denaturant. Furthermore, both *Tt*CutA1 and *Os*CutA1 had considerably good heat reversibility, resulting in producing thermodynamic parameters of high quality, although their denaturation temperatures were high, respectively 113 and 97 °C at pH 7.0. Because the refolding curves of the three proteins seemed to attain constant values, they could be analyzed assuming the equilibrium of ($N_3 \leftrightarrow 3U$). As shown in Figure 6, unfolding ΔG_{H2O} values from the denaturant experiments with *Tt*CutA1 and *Os*CutA1 agreed with those at the same temperature from DSC experiments when using ΔC_p values estimated from the parameters of Spolar et al. (*34*), suggesting that the denaturant data are of high quality.

Therefore, the temperature function of the unfolding ΔG for *Ph*CutA1 could be depicted, as shown in red curves of Figure 6, combining the denaturation temperature from DSC with denaturant data at neutral pH. This stability curve as a function of temperature is important to elucidate the thermodynamic mechanism of protein stability (*36*−*38*) The estimated ΔH value of *Ph*CutA1 at 97.3 °C, which is the T_d of *Os*CutA1 at pH 7.0, was the lowest among the three proteins (Table 2), indicating that the higher stability of *Ph*CutA1 than that of the other two proteins is caused by entropic effects. These findings are reliable because they were compared near the denaturation temperatures of *Tt*CutA1 and *Os*CutA1, and the ΔH values at 97.3 °C of *Ph*CutA1 estimated from the two different values of ΔC_p were quite close (Table 2). It has been reported from DSC experiments that the higher stability of the tryptophan synthase α-subunit from a hyperthermophile, *P. furiosus*, is caused by entropic factors (*20*). Because these proteins are stabilized by many ion pairs, the hydration of charged residues with water upon denaturation might contribute to a decrease in entropy. The unfolding ΔG of *Ph*CutA1 at pH 7.0 and at a protein concentration of 0.02 mM can be estimated to be 202, 245, and 96 kJ/mol at 97.3, 62.5, and 0 °C, respectively, from the red solid curve of Figure 6. The ΔG at 62.5 °C is the highest value. These values of ΔG over all the temperatures are remarkably high compared with reported values (Thermodynamic database for proteins and mutants (*39*)). Compared to the other two CutA1 proteins, *Ph*CutA1 was thermodynamically stable throughout the temperature range, i.e., it has a higher ΔG value than the others at every temperature (Figure 6).

The denaturation temperature of *Os*CutA1 from rice plant with an optimum growth temperature of 28 °C was close to 100 °C at pH 7.0, the structure of which is similar to that of the other two ones (in preparation). The trimeric structures of the three CutA1 proteins are the result of tightly intertwined interactions among the three β-strands. Present experimental results indicate that the unique trimeric structure is responsible for the high stability of mesophilic *Os*CutA1. Recently, we found that CutA1 from *E. coli*, a mesophile, has a denaturation temperature greater than 90 °C at pH 7 (not shown), the structure of which is also similar to that of *Ph*CutA1 (*40*). In the present state, we cannot explain why CutA1s from mesophiles have an unusually high stability.

These results, however, indicate that the unusually high stability of *Ph*CutA1 basically originates from a common trimer structure of the three proteins. On the other hand, at acidic pH, the stabilities of *Tt*CutA1 to heat and a denaturant became higher than those of *Ph*CutA1, which is opposite to those at neutral pH. The analyses of stability factors from the crystal structures of both proteins have indicated that the remarkably increased number of ion pairs in the monomeric structure contributes to the stabilization of *Ph*CutA1 (*1*). At acidic pH, the stability of *Ph*CutA1 might be inferior to that of *Tt*CutA1 because these ion pairs are protonated. Present results confirm the previous explanation that the number of ion pairs plays an important role in enhancing the T_d, up to 150 °C, for *Ph*CutA1.

ACKNOWLEDGMENT

We thank Ms. Miyo Sakai (Institute for Protein Research, Osaka University) for performing experiments on Bechman XL-A.

REFERENCES

1. Tanaka, T., Sawano, M., Ogasahara, K., Sakaguchi, Y., Bagautdinov, B., Katoh, E.,Kuroishi, C., Shinkai, A., Yokoyama, S., and Yutani, K. (2006) Hyper-thermostability of CutA1 protein, with a denaturation temperature of nearly 150 °C, *FEBS Lett. 580*, 4224−4230.
2. Petsko, G. A. (2001) Structural basis of thermostability in hyperthermophilic proteins, or "There's more than one way to skin a cat", *Methods Enzymol. 334*, 469−478.
3. Haney, P. J., Badger, J. H., Buldak, G. L., Reich, C. I., Woese, C. R., and Olsen, G. J. (1999) Thermal adaptation analyzed by comparison of protein sequences from mesophilic and extremely thermophilic *Methanococcus* species, *Proc. Natl. Acad. Sci. U.S.A. 96*, 3578−3583.
4. Honig, B., and Yang, A.-S. (1995) Free energy balance in protein folding, *Adv. Protein Chem. 46*, 27−58.
5. Waldburger, C. D., Schildbach, J. F., and Sauer, R. T. (1995) Are buried salt bridges important for protein stability and conformational specificity?, *Nat. Struct. Biol. 2*, 122−128.
6. Ogasahara, K., Lapshina, E. A., Sakai, M., Izu, Y., Tsunasawa, S., Kato, I., and Yutani, K. (1998) Electrostatic Stabilization in Methionine Aminopeptidase from Hyperthermophile *Pyrococcus furiosus*, *Biochemistry 37, 5939−5946.*
7. Vetriani, C., Maeder, D. L., Tolliday, N., Yip, K. S., Stillman, T. J., Britton, K. L., Rice, D. W., Klump, H. H., and Robb, F. T. (1998) Protein thermostability above 100 °C: a key role for ionic interactions, *Proc. Natl. Acad. Sci. U.S.A. 95*, 12300−12305.
8. Takano, Tsuchimori, K., Yamagata, K., Y., and Yutani, K. (2000) Contribution of Salt Bridges near the Surface of a Protein to the Conformational Stability, *Biochemistry 39*, 12375−12381.
9. Perl, D., Mueller, U., Heinemann, U., and Schmid, F. X. (2000) Two exposed amino acid residues confer thermostability on a cold shock protein, *Nat. Struct. Biol*., *7*, 380−383.
10. Sanchez-Ruiz, J. M., and Makhatadze, G. I. (2001) To charge or not to charge?, *Trends Biotechnol. 19*, 132−135.
11. Makhatadze, G. I., Loladze, V. V., Gribenko, A. V., Lopez, M. M.(2004) Mechanism of thermostabilization in a designed cold shock protein with optimized surface electrostatic interactions, *J. Mol. Biol. 336*, 929−942.
12. Robinson-Rechavi, M., Alibés, A., and Godzik, A. (2006) Contribution of Electrostatic Interactions, Compactness and Quaternary Structure to Protein Thermostability: Lessons from Structural Genomics of *Thermotoga maritime*, *J. Mol. Biol. 356*, 547−557.
13. Pace, C. N. (2000) Single surface stabilizer, *Nat. Struct. Biol. 7*, 345−346.
14. Pace, C. N., Alston, R. W., and Shaw, K. L. (2000) Charge-charge interactions influence the denatured state ensemble and contribute to protein stability, *Protein Sci. 9*, 1395−1398.
15. Jaenicke, R., and Bohm, G. (2001) Thermostability of proteins from *Thermotoga maritima*, *Methods Enzymol. 334*, 438−469.
16. Rees, D. C. (2001) Crystallographic analyses of hyperthermophile proteins, *Methods Enzymol. 334*, 423−437.
17. Ogasahara, K., Nakamura, M., Nakura, S., Tsunasawa, S., Kato, I., Yoshimoto, T., and Yutani, K. (1998) The unusually slow unfolding rate causes the high stability of pyrrolidone carboxyl peptidase from a hyperthermophile, *Pyrococcus furiosus*: equilibrium and kinetic studies of guanidine hydrochloride-induced unfolding and refolding, *Biochemistry 37*, 17537−17544.
18. Kaushik, J. K., Ogasahara, K., and Yutani, K. (2002) The unusually slow relaxation kinetics of the folding-unfolding of pyrrolidone carboxyl peptidase from a hyperthermophile, *Pyrococcus furiosus*, *J. Mol. Biol. 316*, 991−1003.
19. Iimura, S., Yagi, H., Ogasahara, K., Akutsu, H., Noda, Y., Segawa, S., and Yutani, K. (2004) Unusually Slow Denaturation and Refolding Processes of Pyrrolidone Carboxyl Peptidase from a Hyperthermophile are Highly Cooperative: Real-Time NMR Studies, *Biochemistry 43*, 11906−11915.
20. McCrary, B. S., Edmondson, S. P., and Shriver, J. W. (1996). Hyperthermophile protein folding thermodynamics: differential scanning calorimetry and chemical denaturation of Sac7d, *J. Mol. Biol*. *264*, 784−805.
21. Knapp, S., Karshikoff, A., Berndt, K. D., Christova, P., Atanssov, B., and Ladenstein, R. (1996). Thermal unfolding of the DNA-binding protein Sso7d from the hyperthermophile *Sulfolobus solfataricus, J. Mol. Biol*. *264*, 1132−1144.
22. Yamagata, Y., Ogasahara, K., Hioki, Y., Lee, S. J., Nakagawa, A., Nakamura, H., Ishida, M., Kuramitsu, S., and Yutani, K. (2001) Entropic Stabilization of the Tryptophan Synthase α-Subunit from a Hyperthermophile, *Pyrococcus furiosus*: X-ray Analysis and Calorimetry, *J. Biol. Chem*. *276*, 11062−11071.
23. Pace, C. N., Vajdos, F., Fee, G., Grimsley, G., and Gray, Y. (1995) How to measure and predict the molar absorption coefficient of a protein, *Protein Sci. 4*, 2411−2423.
24. Kidokoro, S., Uedaira H., and Wada, A (1988) Determination of thermodynamic functions from scanning calorimetry data. II. For the system that includes self-dissociation/association process, *Biopolymers 27*, 271−297.
25. Tsunoda, Y., Sakai, N., Kikuchi, K., Katoh, S., Akagi, K., Miura-Ohnuma, J., Tashiro, Y., Murata, K., Shibuya, N. and Katoh, E. (2005) Improving expression and solubility of Rice proteins produced as fusion proteins in *Escherichia coli*, *Protein Expression Purif. 42*, 268−277.
26. Backmann, J., Schäfer, G., Wyns, L., and Bonisch, H. (1998) Thermodynamics and kinetics of unfolding of the thermostable trimeric adenylate kinase from the archaeon Sulfolobus acidocaldarius, *J. Mol. Biol. 284*, 817−833.
27. Durchschlag, H. (1986) Specific volumes of biological macromolecules and some other molecules of biological interest, in *Thermodynamic Data for Biochemistry and Biotechnology* (Hinz, H.-J., Ed.) pp 45−128, Springer-Verlag, Berlin, Germany.
28. Tanaka, Y., Tsumoto, K., Nakanishi, T., Yasutake, Y., Sakai, N., Yao, M., Tanaka, I., and Kumagai, I. (2004) Structural implications for heavy metal-induced reversible assembly and aggregation of a protein: the case of *Pyrococcus horikoshii* CutA, *FEBS Lett. 556*, 167−174.
29. Woody, R. W. (1994) Contributions of tryptophan side chains to the far-ultraviolet circular dichroism of proteins, *Eur. Biophys. J. 23*, 253−262.
30. Sinclair, J. F., Ziegler, M. M., and Baldwin, T. O. (1994) Kinetic partitioning during protein folding yields multiple native states, *Nat. Struct. Biol. 1*, 320−326.
31. Lai, Z., McCulloch, J., Lashuel, H. A., and Kelly, J. W. (1997) Guanidine hydrochloride-induced denaturation and refolding of transthyretin exhibits a marked hysteresis: equilibria with high kinetic barriers, *Biochemistry 36*, 10230−10239.
32. Zhu, L., Fan, Y. X., and Zhou, J. M. (2001) Identification of equilibrium and kinetic intermediates involved in folding of urea-denatured creatine kinase, *Biochim. Biophys. Acta 1544*, 320−332.
33. Murphy, K. P., and Freire, E. (1992) Thermodynamics of structural stability and cooperative folding behavior in proteins, *Adv. Protein Chem. 43*, 313−361.
34. Spolar, R. S., Livingstone, J. R, and Record, M. T. Jr. (1992) Use of liquid hydrocarbon and amide transfer data to estimate contributions to thermodynamic functions of protein folding from the removal of nonpolar and polar surface from water, *Biochemistry 31*, 3947−3955.

35. Becktel, W. J., and Schellman, J. A. (1987) Protein stability curves, *Biopolymers 26*, 1859−1877.
36. Nojima, H., Hon-Nami, K., Oshima, T., and Noda, H. (1978). Reversible thermal unfolding of thermostable cytochrome c-552, *J. Mol. Biol. 122*, 33−42.
37. Beadle, B. M., Baase, W. A., Wilson, D. B., Gilkes, N. R., and Shoichet, B. K. (1999) Comparing the thermodynamic stabilities of a related thermophilic and mesophilic enzyme, *Biochemistry 38*, 2570−25766.
38. Deutschman, W. A., and Dahlquist, F. W. (2001) Thermodynamic basis for the increased thermostability of CheY from the hyperthermophile *Thermotoga maritime*, *Biochemistry*, *40*, 13107−13113.
39. Bava, K. A., Gromiha, M. M., Uedaira, H., Kitajima, K., and Sarai, A. (2004) ProTherm, version 4.0: thermodynamic database for proteins and mutants, *Nucleic Acids Res. 32*, D120−D121.
40. Arnesano, F., Banci, L., Benvenuti, M., Bertini, I., Calderone, V., Mangani, S., and Viezzoli. M. S. (2003) The evolutionarily conserved trimeric structure of CutA1 proteins suggests a role in signal transduction, *J. Biol. Chem. 278*, 45999−46006.

BI701761M